DNase I Susceptibility of Bent DNA and Its Alteration by Ditercalinium and Distamycin†

Roberto Mendoza,* Judith Markovits, Jean-Pierre Jaffrezou, Gabriel Muzard, and Jean-Bernard Le Pecq‡
Laboratoire de Pharmacologie Moléculaire, URA 147 du CNRS, U 140 de l'INSERM, Institut Gustave-Roussy, 94805 Villejuif Cedex, France

Received November 28, 1989; Revised Manuscript Received February 2, 1990

ABSTRACT: The bending of kinetoplast DNA from *Crithidia fasciculata* is thought to be related to the periodic distribution of AA or TT cluster sequences. The sensitivity to DNase I of the two strands of this DNA was analyzed at nucleotide resolution by sequencing gel electrophoresis. The effect on the DNase I cleavage pattern of two drugs, ditercalinium and distamycin, that are able to remove bending was analyzed. The same analysis was done on a pBR 322 DNA fragment of random sequence as a control. The periodic distribution of the AA or TT clusters in the bent DNA fragment was first analyzed by computing the autocorrelation function of the AA or TT clusters in the bent DNA fragment. It is shown that the AT tracts are on average 10.5 base pairs apart. This value is almost identical with that of the B-DNA helix pitch in solution [10.5 (Wang, 1979); 10.6 ± 0.1 (Rhodes & Klug, 1980)]. To reveal the periodic pattern of DNase I cleavage on this bent DNA, alone or in presence of drugs, the cross correlation between the different bands obtained from DNAse I cleavage and the presence of AA or TT sequences was computed. This shows that GC and mixed sequences are the most sensitive regions. These data also suggest that there is a periodic fluctuation in the width of the minor groove in the bent fragment. Ditercalinium and distamycin alter the DNase I cutting pattern of the bent DNA fragment but in an inverse fashion. Distamycin protects the AT tract from DNase I attack and enhances DNase I sensitivity of GC and mixed-sequence regions, whereas ditercalinium protects GC and mixed-sequence regions and enhances AT tract DNase I sensitivity. The behavior of the two strands is strikingly asymmetrical in the presence of ditercalinium. At several sequences DNase I sensitivity of the A-rich strand is strongly enhanced, whereas DNase I sensitivity of the corresponding sequence on the T-rich strand is completely protected.

DNA fragments containing sequences that induce bending have been recently isolated from both prokaryotes and eukaryotes (Marini et al., 1982; Wu & Crothers, 1984; Griffith et al., 1986; Kitchin et al., 1986; Linial & Shlomai, 1987). The presence of bent regions in DNA may facilitate the recognition and binding of proteins and eventually of small molecules to these regions (Drew & Travers, 1984; Diekmann, 1987). In addition, proteins that induce or enhance bending of DNA have been characterized. They may play a critical role by inducing structural alterations that are required for initiation of DNA replication, DNA transcription, and compaction (Zahn & Blattner, 1985a,b, 1987; Koepsel & Khan, 1986; Snyder et al., 1986; Hertz et al., 1987; Malkas & Baril, 1989).

Although the role played by bent DNA in gene regulation is not yet completely understood (Lilley, 1986; Welter et al., 1989), the mechanism of DNA bending has been the subject of extensive structural studies (Koo & Crothers, 1986, 1988; Ulanovsky et al., 1986; Ulanovsky & Trifonov, 1987; Diekmann et al., 1987; Zinkel & Crothers, 1987; Allewell, 1988; Burkhoff & Tullius, 1988; Leroy et al., 1988; Yoon et al., 1988; Nadeau & Crothers, 1989; Rice & Crothers, 1989).

Previous works from our laboratory have shown that the antitumor ditercalinium (NSC 366241) (Figure 1), a 7*H*-pyridocarbazole dimer, results in the formation of a high-affinity noncovalent DNA complex in vitro and provokes DNA distortion, which are recognized by the *uvr* ABC repair system of *Escherichia coli* (Roques et al., 1979; Pelaprat et al., 1980; Esnault et al., 1984; Le Pecq & Roques, 1986; Markovits et al., 1986; Lambert et al., 1988, 1989; Segal-Bendirdjian et al., 1988).

Studies performed by ^{31}P and ^{1}H NMR on oligonucleotides have shown that the rigid bipiperidine linker of ditercalinium binds in the major groove of the helix and induces DNA conformational changes upon bis intercalation (Delbarre et al., 1987; Delepierre et al., 1988).

Distamycin (Figure 1) is a naturally occurring oligopeptide antibiotic that binds specifically at AT-rich DNA regions in the minor groove (Van Dyke et al., 1982, Van Dyke & Dervan, 1983; Fox & Waring, 1984; Dervan, 1986; Portugal & Waring, 1987). The structure of an oligonucleotide–distamycin complex has been determined by X-ray crystallography (Coll et al., 1987).

Both distamycin and ditercalinium are able to remove the curving of kinetoplast bent DNA (Wu & Crothers, 1984; Muzard et al., unpublished results of our laboratory). It was therefore of interest to determine whether the uncurving effect of these two drugs is associated with the recognition of DNA sequences on kinetoplast DNA and/or with a specific alteration of DNA structure.

To investigate these problems, DNase I footprinting was used. This method combines enzymatic cleavage of DNA with analysis of the products by sequencing gels. Sites at which the drug is bound are protected from cleavage and are visualized at nucleotide resolution as gaps in the autoradiograph of a denaturing polyacrylamide gel, revealing the position and

† This work was partly supported by grants from Mexico by CONACYT (43573) and in France by CEFI International, INSERM, CNRS, Université Pierre et Marie Curie (Paris VI), as well as Ligue National Contre le Cancer, Association pour la Recherche Contre le Cancer, and Fondation pour la Recherche Médicale.

* To whom correspondence should be addressed.
‡ Present address: Rhône Poulenc Santé, Centre de Recherche de Vitry, BP 14 94403 Vitry-sur-Seine Cedex, France.

0006-2960/90/0429-5035$02.50/0

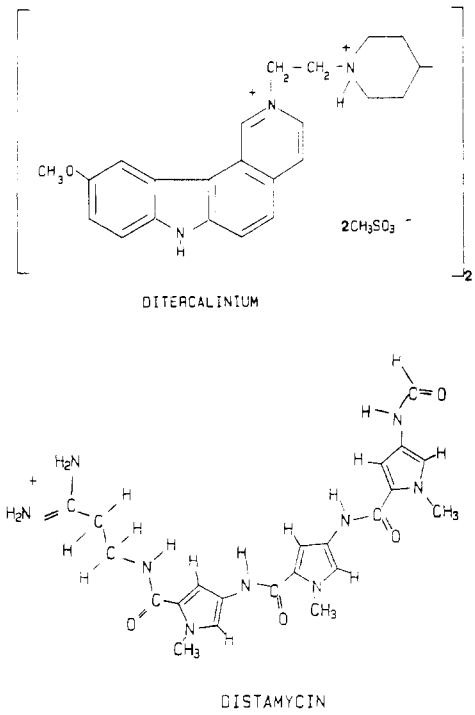

FIGURE 1: Structures of the compounds studied.

length of each ligand binding site (Galas & Schmitz, 1978; Schmitz & Galas, 1979; Maxam & Gilbert, 1980; Goodisman & Drabrowiak, 1985). In addition, the appearance of enhanced or inhibited DNase I cleavage at specific sequences permits the detection of DNA structural alterations.

Materials and Methods

Drugs. Ditercalinium (2,2′-([4,4′-bipiperidine]-1,1′-diyldi-2,1-ethanediyl)bis[10-methoxy-7*H*-pyrido[4,3-*c*]carbazolium] tetramethanesulfonate) was from the Roger Bellon Laboratory. Distamycin was obtained from Sigma. Drug solutions were freshly prepared in water and then sterilized by filtration through a 0.2-μm polycarbonate membrane (Nucleopore, Corp., Peasanton, CA). Ditercalinium concentrations were determined spectrophotometrically at 262 nm (ϵ_{262} = 65 000 M^{-1} cm^{-1}). These solutions were stored at 4 °C in the dark and diluted to appropriate concentrations immediately before use in 10 mM Tris-HCl buffer, pH 7.5, containing 10 mM NaCl.

Enzymes and Nucleotides. Deoxyribonuclease I (DNase I) was obtained from Sigma and prepared as a 7200 unit/mL stock solution in 0.15 M NaCl containing 1 mM $MgCl_2$. This solution was stored at −20 °C and diluted to working concentrations immediately before use. Restriction endonucleases, calf intestinal alkaline phosphatase, and Klenow enzyme were from Boehringer Mannheim. T4 polynucleotide kinase was obtained from New England Biolabs. These enzymes were used in accordance with supplier specifications. [α-^{32}P]dCTP and [γ-^{32}P]dATP, which have a specific activity of 3000 Ci/mmol, were purchased from Amersham.

DNA Substrates. Plasmid pPK 201/CAT from *Crithidia fasciculata* kDNA minicircle containing the bent DNA structure was supplied by Paul T. Englund (Department of Biological Chemistry, The Johns Hopkins University School of Medicine, Baltimore, MD). The 255 base pair (bp) fragment that contains the bent 211-bp DNA was prepared by digesting pPK 201/CAT DNA with *Ava*I–*Hin*dIII restriction endonucleases. This fragment was separated from the larger DNA by FPLC, using a mono Q HR5/5 anion exchange column from Pharmacia Fine Chemicals.

The 255-bp *Ava*I–*Hin*dIII fragment was treated first with alkaline phosphatase and then 5′-end labeled with [γ-^{32}P]-dATP and T4 polynucleotide kinase, whereas it was 3′-end labeled with [α-^{32}P]dCTP and the Klenow fragment of DNA polymerase I. A second enzymatic digestion with the restriction endonuclease *Xba*I yielded two singly 5′- (or 3′-) end labeled fragments 234 and 21 bp long. There was no interference from the smaller fragment because it migrates out of the sequencing gel.

Plasmid pBR 322 DNA was obtained from Boehringer Mannheim. A 375-bp *Eco*RI–*Bam*HI fragment was cleaved from pBR 322. This fragment was separated from the large DNA fragment by FPLC, using a mono Q HR5/5 anion exchange column from Pharmacia Fine Chemicals.

The 375-bp *Eco*RI–*Bam*HI fragment was treated with alkaline phosphatase and then with [γ-^{32}P]dATP and T4 polynucleotide kinase in order to label the 5′-end. The 3′-end labeling was performed with [α-^{32}P]dGTP and the Klenow fragment of DNA polymerase I. Following a secondary cleavage with *Hin*dIII, the 375-bp fragment yielded two singly end labeled fragments 29 and 346 bp long. The smaller fragment was immediately eliminated from the sequencing gel.

All DNA fragments were purified with phenol–chloroform, precipitated with ethanol, and redissolved in TE buffer (10 mM Tris-HCl, 0.1 mM EDTA, pH 7.5) before footprinting analyses (Maniatis et al., 1982).

DNase I Footprinting. Reaction mixtures for footprinting experiments contained 18 μL of 10 mM Tris-HCl (pH 7.5), 20 mM NaCl, 2 mM $MgCl_2$, 2 mM $MnCl_2$, 20 000–30 000 cpm (Cerenkov) of labeled DNA ($\approx$0.8 μM base pairs), and the desired concentration of drug (ditercalinium, 0.25–2 μM; distamycin, 2 and 10 μM). Following equilibration at 20 °C for 60 min, the DNase I (0.01 unit/mL) cleavage reaction was carried out at 4 °C for 3 min and then stopped by addition of EDTA (50 mM final concentration). The DNA was precipitated with ethanol, redissolved in loading buffer [80% formamide, TBE buffer (89 mM Tris–borate, 89 mM boric acid, 2 mM EDTA, pH 8.0), 10 mM Na_2EDTA, 0.1% bromophenol blue, and 0.1% xylene cyanol]. Samples were heated at 90 °C for 5 min prior to electrophoresis. Sequence analysis was performed according to the chemical modification method of Maxam and Gilbert (1980).

Gel Electrophoresis. The products of DNase I digestion and of Maxam–Gilbert reactions were analyzed on 0.3-mm 8% (w/v) polyacrylamide gels containing 7 M urea and TBE buffer, pH 8.0. After 2–4 h of electrophoresis at 1500 V, the gel was soaked in 10% acetic acid for 10 min, dried at 80 °C, and subjected to autoradiography at −70 °C with an intensifying screen.

Densitometry and Data Processing. Autoradiographs were scanned by an MK III C double-beam recording microdensitometer (Joyce, Loebl and Co., Ltd., Gateshead-on-Tyne II, United Kingdom) to produce profiles from which the relative intensity of each band was measured. The value of $OD_{drug-DNA}/OD_{DNA} - 1$ was computed in order to represent the data from this analysis. $OD_{drug-DNA}$ and OD_{DNA} correspond to the optical density of a band obtained from DNase I digestion in the presence and the absence of drug, respectively. This value will be referred to in the paper as the differential cleavage index for each band. The results are displayed on an arithmetic scale. Positive values of the differential cleavage index indicate bonds at which cleavage is enhanced (a value of 1 corresponds to a 2-fold increase in cleavage); negative values of the differential cleavage index

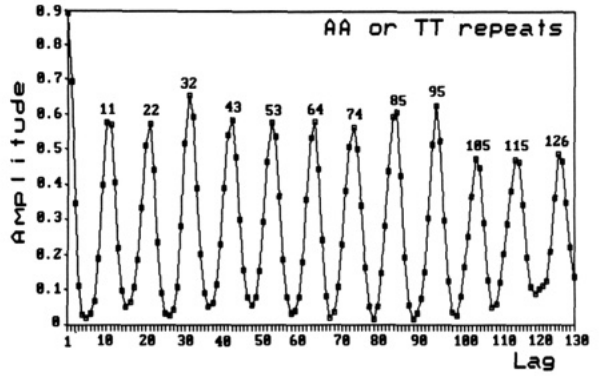

FIGURE 2: Autocorrelation plot of AA or TT occurrences of the 234-bp pPK 201/CAT *AvaI–XbaI* restriction fragment containing the 211-bp bent DNA from *C. fasciculata*.

indicate drug-induced protection (a value of −1 corresponds to complete protection).

Cross-Correlation and Autocorrelation Analysis. The cross correlation between the data obtained from DNase I digestion in the presence and the absence of drug and the occurrences of the AA or TT dinucleotide sequence was computed from

$$\text{Corr } (X,Y)_j = (\sum_i X_{i+j}Y_i)/N$$

which is the discrete form of the classical cross-correlation function. $i = 0, 1, 2, \ldots$ refers to the number of the band on the autoradiograph and $j = 0, 1, 2, \ldots$ to the lag between X and Y.

For the analysis of the DNase I cleavage pattern in the absence of drug, X_i is the optical density of the ith band on the autoradiograph. For the analysis of the DNase I cleavage pattern in the presence of drug, X_i is the differential cleavage index as defined above.

Because the repeat of the AA or TT cluster was to be analyzed, the following coding was used. Y_i is set to 0 if the dinucleotide sequence at the ith position is not found or if it is isolated. If the sequence is in a cluster of three or more identical nucleotides, Y_i is the number of nucleotides which separates the sequence from the closest nucleotide different from those in the cluster.

The following autocorrelation functions were similarly computed:

$$\text{Corr } (X,X)_j = (\sum_i X_{i+j}X_i)/N$$

$$\text{Corr } (Y,Y)_j = (\sum_i Y_{i+j}Y_i)/N$$

RESULTS

In order to characterize the periodicity of the AA and TT cluster repeat in the bent fragment, the autocorrelation of the AA or TT distribution was computed as described under Materials and Methods. If the function repeats itself at given intervals, this will appear as peaks for the corresponding lags. The results of such a computation are shown in Figure 2 with peaks at 11, 22, 33, ..., 105, 115, 126.

An average repeat of 10.5 base pairs for the AT tract is easily deduced from these data. This value is to be compared to the pitch of the B-DNA double helix in solution [10.5 bp (Wang, 1979) and 10.6 ± 0.1 bp (Rhodes & Klug, 1980)].

Figure 3 shows, as an example, an autoradiograph of DNase I cutting patterns of the T-rich strand of the 234-bp bent DNA fragment from pPK 201/CAT in the presence or absence of ditercalinium and distamycin. A 70-bp fragment within the

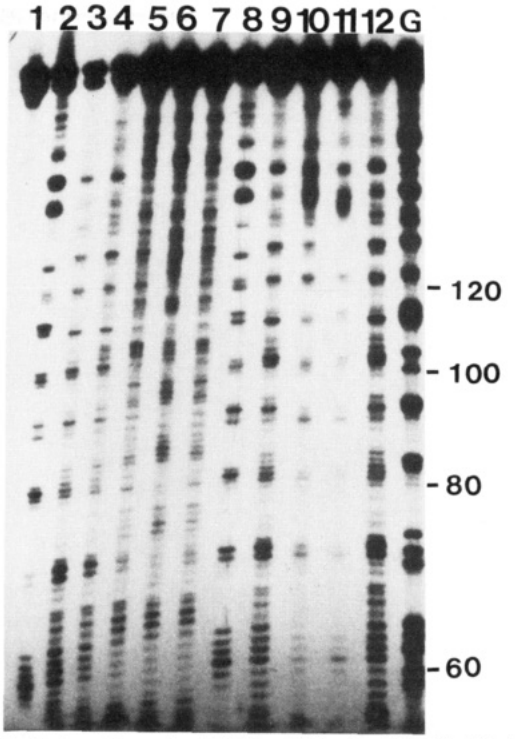

FIGURE 3: Autoradiographs of DNase I digests of the T-rich strand of the 234-bp pPK 201/CAT *AvaI–XbaI* restriction fragment containing the bent DNA from *C. fasciculata* in the absence and the presence of drugs. DNA was 3′-end labeled at the *AvaI* site. Lane 1 is the uncut control DNA. Digestion with DNase I was carried out at 4 °C for 3 min (Lanes 2–8, 10, and 11), 2 min (lane 9), and 1 min (lane 12). Lanes 3, 9, and 12 contained no drug. Lanes 2 and 8 were in the presence of 10 and 2 μM distamycin, respectively. Lanes 4–7 correspond to the presence of 0.25, 0.5, 0.75, and 1 μM ditercalinium, respectively. Lane 10 was in the simultaneous presence of 1 μM ditercalinium and 2 μM distamycin. Lane 11 was in the simultaneous presence of 1 μM ditercalinium and 10 μM distamycin. Lane G shows the pattern resulting from the Maxam–Gilbert dimethyl sulfate–piperidine reaction and indicates the location of guanine residues within the sequence.

234-bp segment is sufficiently well resolved on this gel to be analyzed quantitatively. A slight smearing of the bands is observed when DNA has been incubated with ditercalinium.

As shown in lanes 3, 9, and 12, the most intense bands produced by DNase I cleavage in the absence of drug run at about the same positions as those produced by the Maxam–Gilbert guanine-specific reaction (see lane G).

The densitometer scans presented in Figure 4 show that the DNase I cutting pattern of the T-rich strand (see lane 3 of Figure 3) is clearly sinusoidal at the 5′-end where the most periodic alternation of T_5 and T_6 tracts occurs. Resistance of T tracts to enzyme digestion contrasts with the cutting enhancement of the GC and mixed sequences.

The DNase I cutting pattern of the A-rich strand appears less periodic than that of the T-rich strand; the enzyme also cuts preferentially at the level of the GC-rich regions that separate the A tracts. On both strands, the nucleotide bonds located in the middle of the sequences separating the AT tracts become hypersensitive to DNase I action.

The cross correlation between DNase I cleavage of the bent DNA fragment and the occurrence of AA or TT dinucleotide sequences in the bent DNA fragment was computed in order to quantify the periodic nature of the cutting pattern. The results of the cross correlation between DNase I cleavage in the absence of drug and AA or TT occurrences are shown in Figure 5 for the A-rich (panel A) and T-rich (panel B) strands, respectively. These cross-correlation curves are to be compared

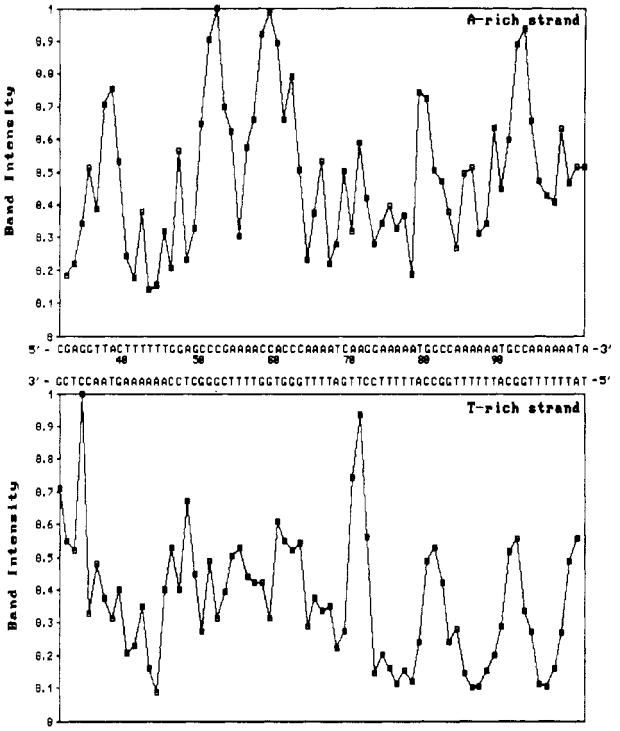

FIGURE 4: Densitometric scans obtained from the autoradiograph of DNase I digestion of 5′- and 3′-end singly-labeled strands of the bent DNA. Sequence positions are represented on the *X* axis and band intensities on the *Y* axis.

with the autocorrelation function of the AA or TT repeats in the same fragment (Figure 5, panel C).

The cross-correlation curve for the A-rich strand shows peaks at positions 5, 15, 25, and 35, similar to that of the T-rich strand (6–7, 17, 26, 36). Both curves show an phase opposite to that of AA or TT autocorrelation. Minima of the DNase I cleavage correspond to maxima in the AA or TT autocorrelation function. This result indicates clearly that the AT tracts of bent DNA are less sensitive to DNase I digestion than other sequences. However, the A-rich strand elicits a less clear periodicity than the T-rich strand.

The DNase I digestion patterns observed in the presence of ditercalinium (lanes 4–7 in Figure 3) become inversed compared to the DNase I digestion pattern observed in the absence of drug. The more intense bands in one pattern become the less intense bands in the other one and vice versa.

In order to analyze the effect of ditercalinium on the DNase I cleavage pattern, intensities of bands from the lanes of the autoradiographs were converted through densitometric measurements into the differential cleavage index as described under Materials and Methods. Figure 6 represents the diagram obtained for both strands of the bent pPK 201/CAT DNA fragment in the presence of 1 μM ditercalinium. On the T-rich DNA strand (lower panel) ditercalinium clearly protects the regions located between T stretches (T_4–T_6 tracts). The size of the protected regions is about six nucleotides. Pronounced cleavage enhancements are observed in the T tracts and especially apparent on the last two analyzed T_6 tracts separated by four nucleotides.

The DNase I digestion pattern of the A-rich strand is quite different. Ditercalinium globally induces a very slight protection of the regions located between A stretches. Surprisingly, the first T_6 tract becomes hypersensitive to DNase I cleavage. DNase I cleavage of the two strands becomes strikingly asymmetric in the presence of ditercalinium.

Figure 7 shows the cross correlation between the DNase I differential cleavage index and the AA or TT occurrences

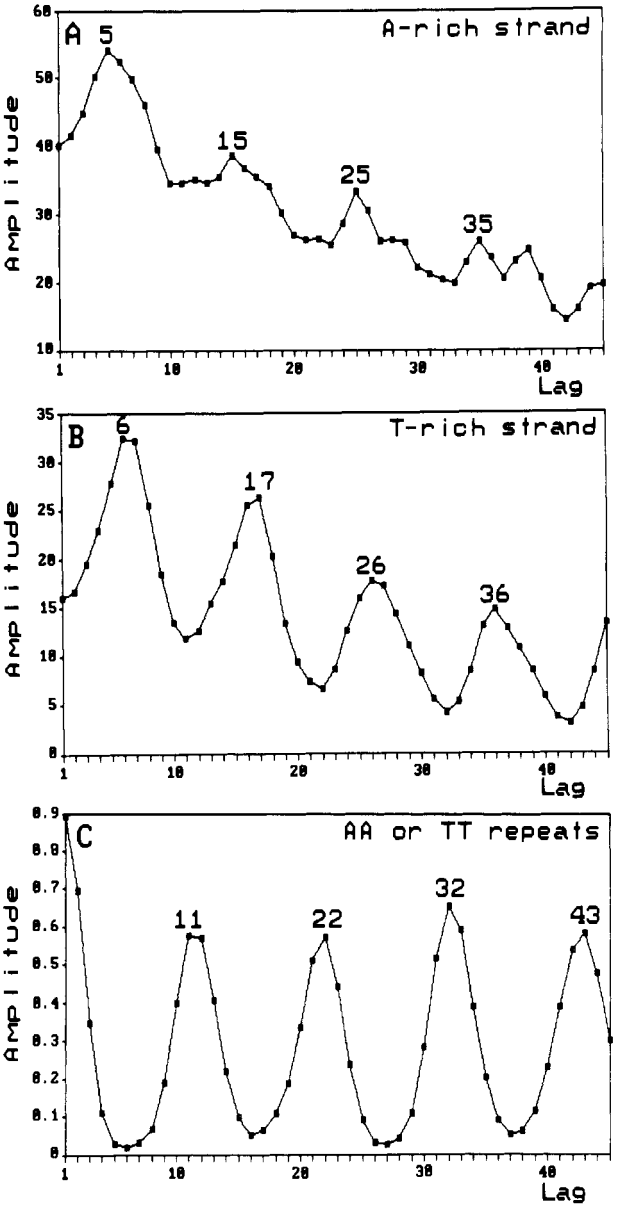

FIGURE 5: Cross-correlation plots between DNase I cutting pattern and AA or TT dinucleotide occurrences on the A-rich (A) and T-rich (B) strands of bent DNA. (C) Autocorrelation of the AA or TT dinucleotide occurrences.

obtained on the A-rich (Figure 7, panel A) and T-rich (Figure 7, panel B) strands in the presence of 1 μM ditercalinium. For the T-rich strand, the cross-correlation function exhibits a clear periodicity (peaks at positions 11, 22, 32, and 42) in phase with that of TT occurrences (Figure 7, panel C). Periodicity for the A-rich strand is not so clear.

We also examined the differential cleavage index of DNase I in the presence of 10 μM distamycin (Figure 8) corresponding to lane 2 of the autoradiograph presented in Figure 3. Protected sites are centered at T-rich regions. Enhancements of cleavage are observed in the GC-rich regions. Widespread protected regions are observed on the A-rich DNA strand. The DNase I cleavage pattern in the presence of distamycin resembles that observed with DNase I alone, but the contrast is enhanced.

Figure 9 shows the cross correlation between the differential DNase I cleavage index and the occurrences of AA or TT in the presence of 10 μM distamycin on the A-rich (Figure 9, panel A) and the T-rich (Figure 9, panel B) strands. The cross-correlation functions for the A-rich strand and the T-rich

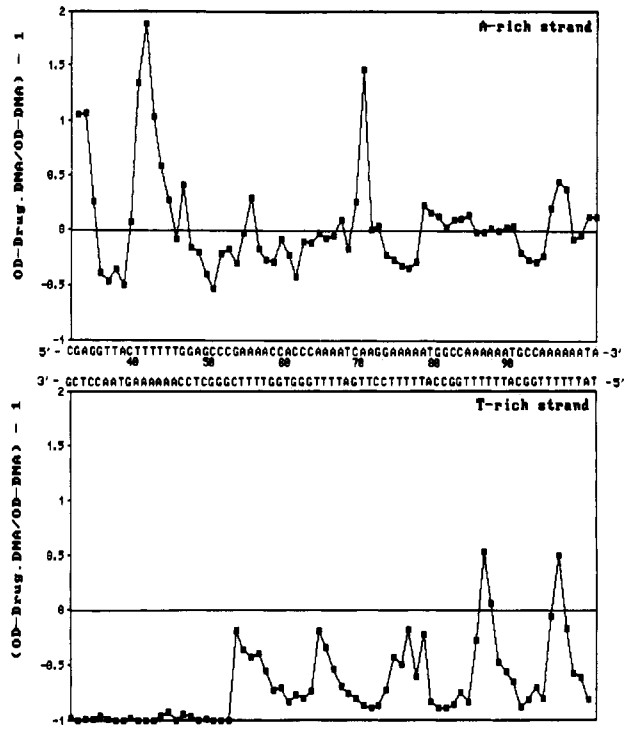

FIGURE 6: DNase I differential cleavage index plots of the two strands of bent DNA fragment in the presence of 1 μM ditercalinium. The sequences of the bent DNA fragments are shown along the abscissa. The differential cleavage index on the ordinate was calculated as described under Materials and Methods. Negative values on the ordinate indicate protection by the bound drug while positive values indicate enhanced cleavage.

strand are slightly different. The periodical repeat is best observed with the T-rich strand as in the ditercalinium case, but the difference in behavior between the two strands is not so marked. The minima of the cross-correlation function correspond to the repeat of the protected regions. They more or less coincide with the AT tract repeats as seen with the autocorrelation function for AA or TT sequences. This indicates that protection is best seen on AT-rich regions, in agreement with distamycin specificity.

The maxima of the cross-correlation function correspond to the periodicity of the most sensitive DNase I regions. This indicates that the 5'-side of the AT tract is the most sensitive DNase I region. The peaks of the cross-correlation function for the T-rich plot are shifted by −3 to −4 nucleotides from those of AA or TT occurrences (Figure 9, panel C).

Therefore, the footprinting experiments in Figure 3 reveal a complementary nature of distamycin and ditercalinium binding. The simultaneous effects of these two drugs at high concentrations (lanes 10 and 11) protect quasi-completely the T-rich DNA strand of the bent pPK 201/CAT DNA fragments from DNase I digestion.

Finally, in order to compare our observations made on bent DNA with those of nonbent DNA, similar DNase I footprinting experiments were performed in the presence of ditercalinium or distamycin with the nonbent *Eco*RI–*Bam*HI 375-bp restriction fragment from pBR 322 DNA.

DNase I differential cleavage plots obtained in the presence of ditercalinium (1 μM) and distamycin (10 μM) are shown in Figures 10 and 11, respectively. No evident relation between sequence and DNase I enhanced or inhibited cleavage is apparent. Cross correlation and autocorrelation for all sequences were computed, and no periodicity was detected (data not shown). However, this DNA fragment contains an AT-rich and a GC-rich region. In the presence of distamycin the AT-rich region is globally protected while the GC-rich region becomes more sensitive to DNase I cleavage. In the presence of ditercalinium this GC-rich region is preferentially protected.

Discussion

The analysis of the AT tract repeat in the bent DNA fragment of the kinetoplast by autocorrelation reveals the extraordinary organization of this sequence. Peaks appears in the autocorrelation function at very regular intervals (11, 22, 33, ..., 126, ...). This shows that the AT tracts repeat on average at exactly 10.5 nucleotides over a long distance, although the AT tracts are not exactly spaced on the bent DNA fragment. This value is almost identical with the pitch of the B-DNA helix in solution (Wang, 1979; Rhodes & Klug, 1980). Such a coincidence between pitch and AA or TT occurrences will cause a perfect in-plane curving of this kinetoplast DNA fragment.

Analysis of the DNase I cleavage pattern by cross-correlation functions also reveals interesting features. General trends can be extracted from the data without interference from the fluctuation of DNase I activity at local sequences. It eliminates possible strong fluctuations at some sequences, which from simple visual inspection may dissimulate the global pattern. The cross correlation between DNase I sensitivity and AA or TT occurrences is almost exactly in an opposite phase to that of AA and TT autocorrelation. This indicates that the maximum sensitivity of DNase I occurs on average in the middle of GC-rich mixed sequences, which separate the AT tracts. DNase I sensitivity analysis of bent kinetoplast DNA provides evidence about the structural periodic fluctuations of this DNA.

DNase I cleavage is determined by the structure of the DNA helix rather than by the sequence per se (Bernardi et al., 1975). Dickerson and Drew (1981) first unraveled the relation between DNA structure and DNase I sensitivity. They noticed a strong correlation between the helix twist angle at the cleavage site and DNase I sensitivity. Structural determination by X-ray crystallography of a DNA octanucleotide–DNase I complex (Oefner & Suck, 1986; Suck & Oefner, 1986; Suck et al., 1988) later allowed a better understanding of the factors controlling the rate of DNase I cleavage. It was observed that the binding between the enzyme and DNA takes place in the minor groove and involves only contacts with the phosphate–sugar backbone of both strands. Bases are not involved in the recognition. It could then be understood that the DNase I rate of cleavage was controlled by DNA structural factors rather than by direct sequence effects. The width of the minor groove is clearly an important parameter. The enzyme would cut best where the minor groove is of average width, as in B-DNA (12 Å), rather than narrow as in homopolymeric tracts of dA·dT or expanded as in tracts of oligo(dG·dC). It was also noticed that DNase I induces a DNA bending of 20° and that the cut takes places on the 3'-side of the bent. Interestingly the bending is toward the large groove whereas the bending induced in the kinetoplast DNA by A tracts is in the opposite direction, that is, toward the minor groove (Salvo & Grindley, 1987; Zinkel & Crothers, 1987). Therefore, it was proposed that DNA located in hypersensitive DNase I regions in the nucleus might be bent toward the major groove (Suck et al., 1988). Because the binding of DNase I to DNA needs a distortion of the DNA minor groove, it was also suggested that the local DNA bending flexibility could be an important determinant in controlling the rate of DNase I action (Suck et al., 1988; Travers, 1989). Recently, the relation between DNA flexibility and DNase I cleavage rate was investigated (Hogan et al., 1989). It was proposed that,

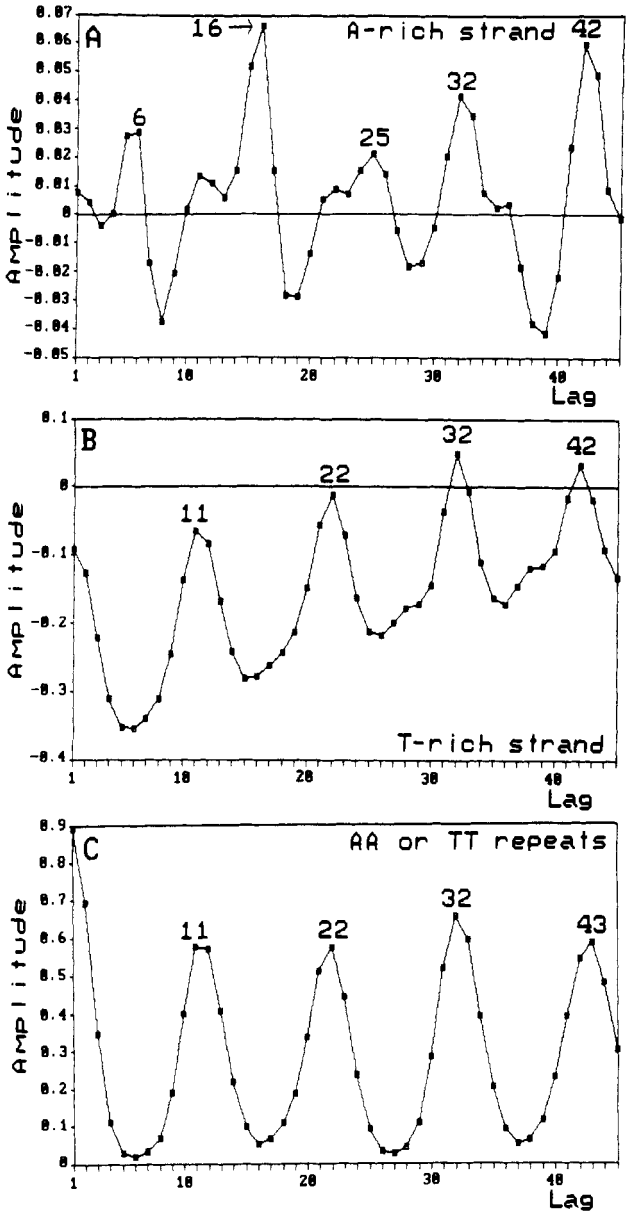

FIGURE 7: Cross-correlation plots between DNase I differential cleavage index and AA or TT occurrences on the A-rich (A) and T-rich (B) strands of bent DNA in the presence of 1 μM ditercalinium. (C) Autocorrelation of AA or TT occurrences.

in absence of significant local variation of DNA secondary structure, the DNase I rate of cleavage is correlated with local bending flexibility. Interestingly, the position of the maximum of the DNase I rate of cleavage is shifted three nucleotides on the 3′-side of the maximum of flexibility.

The bending of kinetoplast DNA is thought to result from an alteration of the DNA structure at the junction of A tract and mixed sequence, on both 5′- and 3′-sides of the A tracts (Haran & Crothers, 1989; Travers, 1989). Our data do not evidence a specific DNA cleavage enhancement at these positions. This is expected since DNA must be bent in the opposite direction to allow DNase I binding (Suck et al., 1988). As discussed above, minor groove width is an important factor for DNase I action. Therefore, our results could indicate that there is a periodic fluctuation of the minor groove width in the bent fragment. Alternatively, A tracts could induce a local destabilization of DNA and increase flexibility between A tracts. To precisely determine the role of the two factors, local measurements of flexibility would be required. NMR studies indicate already that A tracts are associated with anomalous

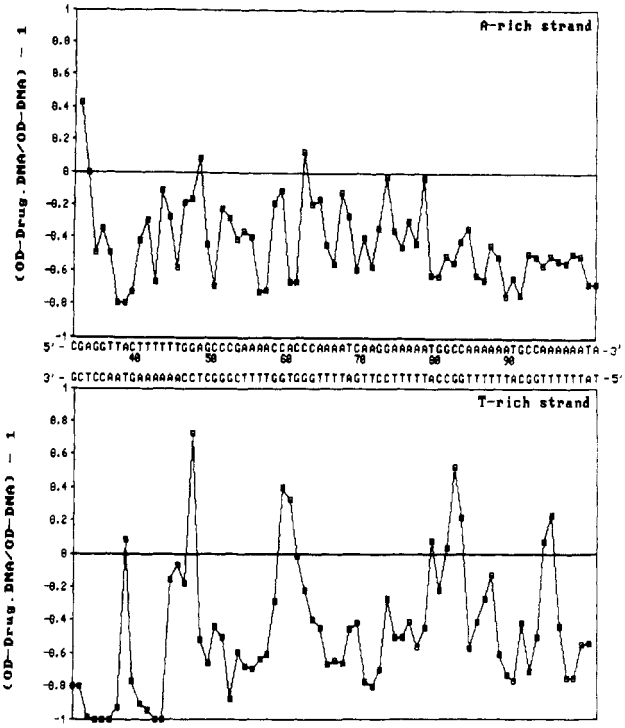

FIGURE 8: DNase I differential cleavage index plots of the two strands of the bent DNA fragment in the presence of 10 μM distamycin. Presentation is as described in the legend of Figure 6.

base pair kinetics (Leroy et al., 1988).

Another interesting aspect of this DNase I sensitivity analysis is the asymmetric behavior of the two DNA strands. Such behavior could result from a differential structure of the A-rich and T-rich strands as proposed in the heteronomous model of DNA (Arnott et al., 1983). These observations are consistent with the structure of B-DNA containing AT tracts as determined by X-ray crystallography (Dickerson, 1983).

Distamycin has been characterized as a molecule that preferentially binds to the minor groove of AT-rich regions of B-DNA. Our DNase I footprinting experiments performed on the bent DNA fragment clearly confirm the AT selectivity of this drug. We observed that distamycin protects A and T tracts on the T-rich strand, whereas treatment of bent DNA with distamycin results in a more global protection of the complementary A-rich strand from the DNase I cleavage. This feature is clearly apparent on the cross-correlation function (Figure 9) where the periodicity is best observed for the T-rich strand. The simplest explanation for these data is that distamycin protects the two strands at positions where it is bound. At a distance it induces DNA alterations, which are asymmetrical for the A-rich and T-rich strands.

DNase I footprinting of B-DNA of random sequences (*Eco*RI–*Hin*dIII restriction fragment from pBR 322) in the presence of ditercalinium does not evidence any clear protected sequences. However, it must be underlined that there are 136 different binding sites for a bifunctional intercalator like ditercalinium (Dervan, 1986). Therefore, the detection of a specific protected sequence would require an extensive statistical analysis of a substantial amount of footprinting data.

In contrast, the binding of ditercalinium to kinetoplast bent DNA induces a periodic DNase I protection of the sequences in between the AT tracts, whereas the AT tracts themselves which were the least sensitive to DNase I become the most sensitive regions in the presence of ditercalinium. The analysis of the cross-correlation function between the differential DNase I cleavage index and the occurrences of AA or TT sequences shows that the periodicity is identical with that of

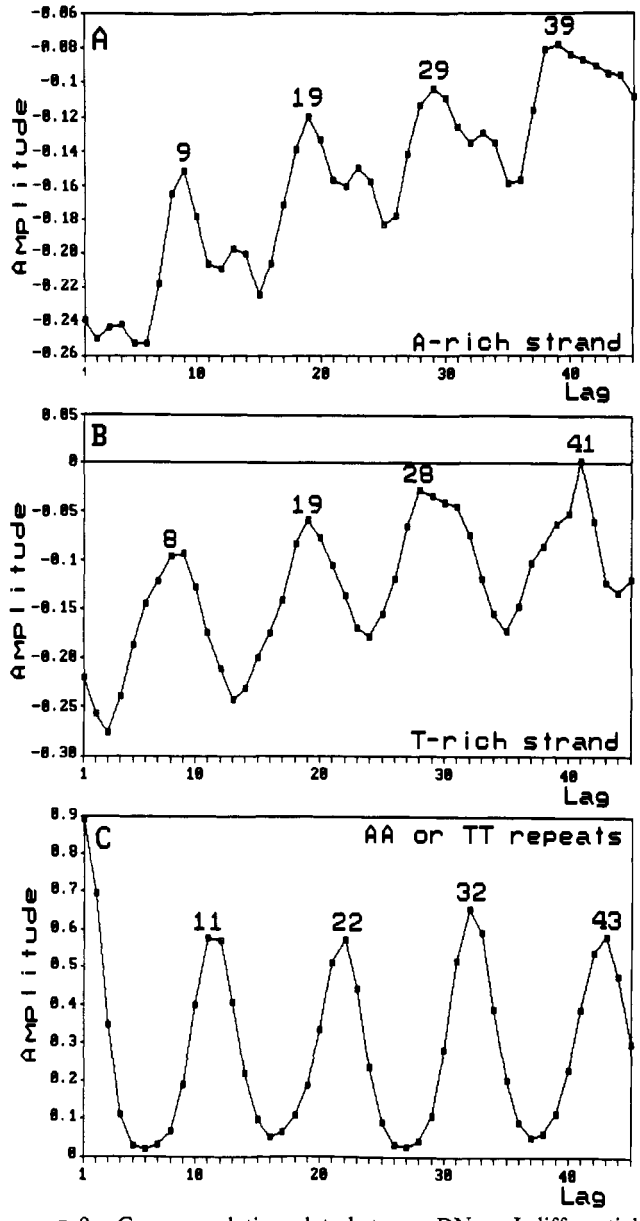

FIGURE 9: Cross-correlation plots between DNase I differential cleavage index and AA or TT occurrences on the A-rich (A) and T-rich (B) strands of bent DNA in the presence of 10 μM distamycin. (C) Autocorrelation of AA or TT occurrences.

the AA or TT sequence repeat for the T-rich strand, but not for the A-rich strand. Furthermore, the phases of the cross-correlation function and the autocorrelation of AA or TT sequence are identical.

The asymmetrical behavior of the A-rich and T-rich strand in the presence of ditercalinium is clearly illustrated by the following observations. As seen in Figure 6, at position 40 a T_6 repeat starts on the A-rich strand, and therefore, an A_6 repeat starts on the T-rich strand. The DNase I sensitivity of the T_6 cluster on the A-rich strand is strongly enhanced, whereas the complementary A_6 cluster on the T-rich strand is completely protected. This apparently surprising result could be rationalized in the following way: Ditercalinium is known to bind to the large groove of DNA. The presence of ditercalinium at a given sequence would not prevent access of DNase I to the small groove of this sequence and its nucleasic attack. Therefore, the differential attack of DNase I would indirectly and only result from the distortion of the narrow groove induced by the presence of ditercalinium in the major groove. In such a case, ditercalinium is not expected to induce a clear footprint on DNA in relation to an eventual specific

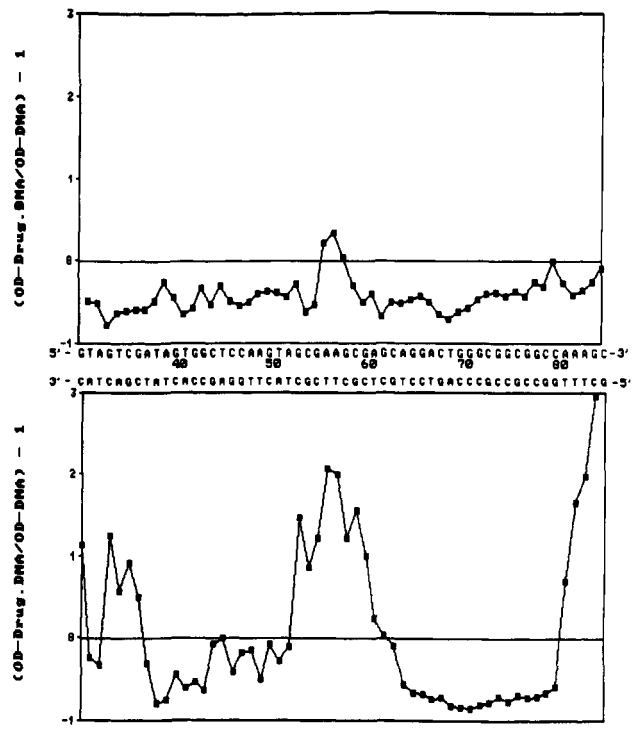

FIGURE 10: DNase I differential cleavage index plots of the two strands of the 346-bp *Hin*dIII–*Bam*HI restriction fragment from pBR 322 in the presence of 1 μM ditercalinium. Presentation is as described in the legend of Figure 6.

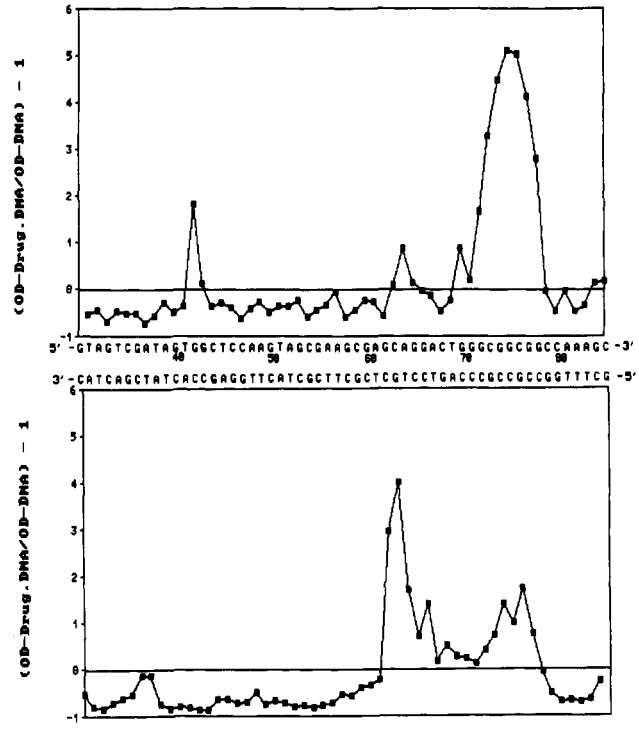

FIGURE 11: DNase I differential cleavage index plots of the 346-bp *Hin*dIII–*Bam*HI restriction fragment from pBR 322 in the presence of 10 μM distamycin. Presentation is as described in the legend to Figure 6.

binding preference of ditercalinium for given sequences. In agreement with this model, it is found that even at a high ditercalinium concentration (1 μM), when DNA is fully saturated by ditercalinium, no complete protection is observed.

The results reveal that ditercalinium induces a strong asymmetrical deformation of the DNA double helix. Such a property could be correlated with the finding of Lambert et al. (1989). These authors demonstrated that the *uvr* ABC

proteins involved in the repair of chemical adducts with DNA recognize the reversible ditercalinium–DNA complex. Since the repair system must selectively recognize the modified strand and not the unmodified one, the asymmetrical nature of the structures at the level of the adducts must be involved in the recognition process.

In conclusion, our results show that the periodic repetition of sequences in DNA could alter DNA structure and reactivity to drugs and proteins. The curving of DNA is the most apparent aspect of this alteration. In addition, the binding of a drug like ditercalinium to such a DNA induces asymmetrical alterations on the two strands. It remains to be determined whether such asymmetrical effects can be induced by DNA binding proteins and whether they are of any importance in biological functions.

ACKNOWLEDGMENTS

We are grateful to Drs. T. O'Connor, B. P. Roques, A. Sarasin, F. Bourre, B. Renê, and A.-J. Sablon for fruitful discussions. We thank J. Gabarro for his kind help in computation analysis and J. Couprie for preparing the pPK 201/CAT DNA.

REFERENCES

Allewell, N. (1988) *Trends Biochem. Sci. 13*, 193–195.
Arnott, S., Chandrasekaran, R., Hall, I. H., & Puigjaner, L. C. (1983) *Nucleic Acids Res. 11*, 4141–4155.
Bernardi, A., Gaillard, C., & Bernardi, G. (1975) *Eur. J. Biochem. 52*, 451–457.
Burkhoff, A. M., & Tullius, T. D. (1988) *Nature 331*, 455–457.
Coll, M., Frederick, C. A., Wang, A. H., & Rich, A. (1987) *Proc. Natl. Acad. Sci. U.S.A. 84*, 8385–8389.
Delbarre, A., Delepierre, M., Garbay, C., Igolen, J., Le Pecq, J. B., & Roques, B. P. (1987) *Proc. Natl. Acad. Sci. U.S.A. 84*, 2155–2159.
Delepierre, M. (1988) *Biopolymers 27*, 957–968.
Dervan, P. B. (1986) *Science 232*, 464–471.
Dickerson, R. E. (1983) *J. Mol. Biol. 166*, 419–441.
Dickerson, R. E., & Drew, H. R. (1981) *J. Mol. Biol. 149*, 761–786.
Diekmann, S., Kitzing, E. V., McLaughlin, L., Ott, J., & Eckstein, F. (1987) *Proc. Natl. Acad. Sci. U.S.A. 84*, 8257–8261.
Drew, H. R., & Travers, A. A. (1984) *Cell 37*, 491–502.
Esnault, C., Roques, B. P., Jacquemin-Sablon, A., & Le Pecq, J. B. (1984) *Cancer Res. 44*, 4355–4360.
Fox, K. R., & Waring, M. J. (1984) *Nucleic Acids Res. 12*, 9271–9285.
Galas, D. J., & Schmitz, A. (1978) *Nucleic Acids Res. 5*, 3157–3170.
Goodisman, J., & Drabrowiak, J. C. (1985) *J. Biomol. Struct. Dyn. 2*, 967–978.
Griffith, J., Bleyman, M., Rauch, C. A., Kitchin, P. A., & Englund, P. T. (1986) *Cell 46*, 717–724.
Haran, T. E., & Crothers, D. M. (1989) *Biochemistry 28*, 2763–2767.
Hertz, G. Z., Young, M. R., & Mertz, J. E. (1987) *J. Virol. 61*, 2322–2325.
Hogan, M. E., Roberson, M. W., & Austin, R. H. (1989) *Proc. Natl. Acad. Sci. U.S.A. 86*, 9273–9277.
Kitchin, P. A., Klein, V. A., Ryan, K. A., Gann, K. L., Rauch, C. A., Kang, D. S., Wells, R. D., & Englund, P. T. (1986) *J. Biol. Chem. 261*, 11302–11309.
Koepsel, R. R., & Khan, S. A. (1986) *Science 233*, 1316–1318.
Koo, H. S., & Crothers, D. M. (1988) *Proc. Natl. Acad. Sci. U.S.A. 85*, 1763–1767.
Koo, H. S., Wu, H., & Crothers, D. M. (1986) *Nature 320*, 501–506.
Lambert, B., Roques, B. P., & Le Pecq, J. B. (1988) *Nucleic Acids Res. 16*, 1063–1078.
Lambert, B., Jones, B. K., Roques, B. P., & Le Pecq, J. B. (1989) *Proc. Natl. Acad. Sci. U.S.A. 86*, 6557–6561.
Le Pecq, J. B., & Roques, B. P. (1986) in *Mechanisms of DNA Damage and Repair: Implications for Carcinogenesis and Risk Assessment* (Simic, M. G., Grossman, L., & Upjon, A., Eds.) pp 219–230, Plenum, New York.
Leroy, J.-L., Charretier, E., Kochoyan, M., & Guêron, M. (1988) *Biochemistry 27*, 8894–8898.
Lilley, D. (1986) *Nature 320*, 487–488.
Linial, M., & Shlomai, J. (1987) *Proc. Natl. Acad. Sci. U.S.A. 84*, 8205–8209.
Malkas, L. H., & Baril, E. F. (1989) *Proc. Natl. Acad. Sci. U.S.A. 86*, 70–74.
Maniatis, T., Fritsch, E. F., & Sambrook, J. (1982) *Molecular Cloning: A Laboratory Manual*, Cold Spring Harbor Laboratory, Cold Spring Harbor, NY.
Marini, J. C., Levence, S. D., Crothers, D. M., & Englund, P. T. (1982) *Proc. Natl. Acad. Sci. U.S.A. 79*, 7674–7688.
Markovits, J., Pommier, Y., Mattern, M. R., Esnault, C., Roques, B. P., Le Pecq, J. B., & Kohn, K. W. (1986) *Cancer Res. 46*, 5821–5826.
Maxam, A. M., & Gilbert, W. (1980) *Methods Enzymol. 65*, 499–560.
Nadeau, J. G., & Crothers, D. M. (1989) *Proc. Natl. Acad. Sci. U.S.A. 86*, 2622–2626.
Oefner, C., & Suck, D. (1986) *J. Mol. Biol. 192*, 605–632.
Pelaprat, D., Delbarre, A., Le Guen, I., Roques, B. P., & Le Pecq, J. B. (1980) *J. Med. Chem. 23*, 1336–1343.
Portugal, J., & Waring, M. J. (1987) *Eur. J. Biochem. 167*, 281–289.
Rhodes, D., & Klug, A. (1980) *Nature 286*, 573–578.
Rice, J. A., & Crothers, D. M. (1989) *Biochemistry 28*, 4512–4516.
Roques, B. P., Pelaprat, D., Le Guen, I., Porcher, G., Gosse, C., & Le Pecq, J. B. (1979) *Biochem. Pharmacol. 28*, 1811–1815.
Salvo, J. J., & Grindley, N. D. (1987) *Nucleic Acids Res. 15*, 9771–9779.
Schmitz, A., & Galas, D. J. (1979) *Nucleic Acids Res. 6*, 111–137.
Segal-Bendirdjian, E., Colaud, D., Roques, B. P., & Le Pecq, J. B. (1988) *Cancer Res. 48*, 4982–4992.
Snyder, M., Buchman, A. R., & Davis, R. D. (1986) *Nature 324*, 87–89.
Suck, D., & Oefner, C. (1986) *Nature 321*, 620–625.
Suck, D., Lahm, A., & Oefner, C. (1988) *Nature 332*, 464–468.
Travers, A. A. (1989) *Annu. Rev. Biochem. 58*, 427–452.
Ulanovski, L. E., & Trifonov, E. N. (1987) *Nature 326*, 720–722.
Ulanovski, L., Bodner, M., Trifonov, E. N., & Choder, M. (1986) *Proc. Natl. Acad. Sci. U.S.A. 83*, 862–866.
Van Dyke, M. W., & Dervan, P. B. (1983) *Nucleic Acids Res. 16*, 5555–5567.
Van Dyke, M. W., Hertzberg, R. P., & Dervan, P. B. (1982) *Proc. Natl. Acad. Sci. U.S.A. 79*, 5470–5474.

Wang, J. C. (1979) *Proc. Natl. Acad. Sci. U.S.A. 76*, 200–203.
Welter, C., Dooley, S., Zang, K. D., & Blin, N. (1989) *Nucleic Acids Res. 17*, 6077–6086.
Wu, H., & Crothers, D. M. (1984) *Nature 308*, 509–513.
Yoon, C., Privé, G. G., Goodsell, D. S., & Dickerson, R. E. (1988) *Proc. Natl. Acad. Sci. U.S.A. 85*, 6332–6336.
Zahn, K., & Blattner, F. R. (1985a) *EMBO J. 4*, 3605–3616.
Zahn, K., & Blattner, F. R. (1985b) *Nature 317*, 451–453.
Zahn, K., & Blattner, F. R. (1987) *Science 236*, 416–422.
Zinkel, S. S., & Crothers, D. M. (1987) *Nature 328*, 178–181.

Pseudomonas aeruginosa Exotoxin A: Alterations of Biological and Biochemical Properties Resulting from Mutation of Glutamic Acid 553 to Aspartic Acid†

Cameron M. Douglas‡,§ and R. John Collier*,‡,‖

Department of Microbiology and Molecular Genetics, Harvard Medical School, 25 Shattuck Street, and Shipley Insitute of Medicine, 200 Longwood Avenue, Boston, Massachusetts 02115

Received November 14, 1989; Revised Manuscript Received January 19, 1990

ABSTRACT: Glutamic acid 553 of *Pseudomonas aeruginosa* exotoxin A (ETA) was identified earlier as a putative active-site residue by photoaffinity labeling with NAD. Here ETA-E553D, a cloned form of the toxin in which Glu-553 has been replaced by aspartic acid, was purified from *Escherichia coli* extracts and characterized. Cytotoxicity of the mutant toxin for mouse L-M cells was less than 1/400 000 that of the wild type. The mutation caused a 3200-fold reduction in NAD:elongation factor 2 ADP-ribosyltransferase activity, as estimated by assays with an active fragment derived from the toxin by digestion with thermolysin. NAD glycohydrolase activity was reduced somewhat less, by a factor of 50, and photoaffinity labeling with NAD by a factor of 2. We detected less than 2-fold change in the values of K_M for NAD or elongation factor 2 and no change in K_D for NAD, as determined by quenching of protein fluorescence. The drastic reduction of ADP-ribosyltransferase activity therefore results primarily from an effect of the mutation on k_{cat}, implying that Glu-553 plays an important and possibly direct role in catalyzing this reaction. The effects of the E553D mutation are similar to those of the E148D mutation in diphtheria toxin, supporting the notion that these two Glu residues perform the same function in their respective toxins.

Exotoxin A of *Pseudomonas aeruginosa* (ETA;[1] 613 residues, M_r 66 583) belongs to a class of bacterial toxins that ADP-ribosylate target proteins of eucaryotic cells (Jacobson & Jacobson, 1989; Collier & Mekalanos, 1980). Like diphtheria toxin (DT), ETA is a proenzyme, which, after activation, catalyzes transfer of the ADP-ribose moiety of NAD to the diphthamide residue of elongation factor 2 (EF-2). This blocks the translocation step of protein synthesis, thereby causing cell death.

Photoaffinity labeling and directed mutagenesis have been used to identify a putative active-site residue of ETA. Carroll and Collier (1987) found that radiolabel from nicotinamide-labeled NAD was efficiently transferred to a single site, position 553, of an enzymically active thermolysin fragment (A_{tl}) of the toxin when the mixture was irradiated with 254-nm ultraviolet light (Carroll & Collier, 1987). The photoproduct at position 553 was chromatographically identical with that formed at position 148 in diphtheria toxin (DT) fragment A irradiated under similar conditions. In the DT fragment Glu-148 was modified to give a photoproduct containing the nicotinamide ring of NAD linked by its carbon 6 to the decarboxylated γ-methylene group (Carroll et al., 1985). The structure of the protoproduct suggests that the carboxyl function may be in contact with the *N*-glycosyl linkage ruptured during ADP-ribosyl transfer and hence directly involved in catalysis.

To probe the role of Glu-553 of ETA in ADP-ribosylation activity, NAD glycohydrolase activity, cytotoxicity, and photolabeling with NAD, we substituted Asp for this residue in cloned ETA and expressed the mutant gene in *Escherichia coli* (Douglas & Collier, 1987). Earlier, ETA was expressed in *E. coli* under control of the hybrid *tac* promoter, and it was found that the gene product, in crude extracts, was indistinguishable from ETA produced by *P. aeruginosa* with regard to toxicity and enzymic activity (Douglas et al., 1987). When the Glu-553 → Asp mutant toxin, ETA-E553D, was expressed in *E. coli* and assayed in crude extracts, its ADP-ribosylation and cytotoxic activities were found to have been reduced by greater than 1800-fold and 10 000-fold, respectively (Douglas & Collier, 1987). Here we report purification and more detailed characterization of ETA-E553D obtained by expression of the mutant cloned gene in *E. coli*.

Experimental Procedures

Bacterial Strains. E. coli JM103 (pCDPT2) and *E. coli* JM103 (pCDPTE553D) were described recently (Douglas et al., 1987; Douglas & Collier, 1987).

Purification of ETA and ETA-E553D from E. coli. Exotoxin A produced by *P. aeruginosa* PA103 was purified as described (Lory & Collier, 1980) and used as a reference throughout these studies. Overnight cultures of *E. coli* JM103 (pCDPT2) and JM103 (pCDPTE553D) in L-broth with 100

† This work was supported by USPHS Grants AI22021 and AI22848 from the National Institute of Allergy and Infectious Diseases.

* To whom correspondence should be addressed at Harvard Medical School.
‡ Harvard Medical School.
§ Present address: Mail Drop R80Y-300, Merck & Co., Inc., P.O. Box 2000, Rahway, NJ 07065.
‖ Shipley Institute of Medicine.

[1] Abbreviations: ETA, *Pseudomonas aeruginosa* exotoxin A; DT, diphtheria toxin; A_{tl}, enzymically active fragment of ETA generated by digestion with thermolysin.

0006-2960/90/0429-5043$02.50/0